ResearchGate

See discussions, stats, and author profiles for this publication at: https://www.researchgate.net/publication/223963972

Structural characterization of electron–induced proton transfer in the formic acid dimer anion, (HCOOH)2−, with vibrational and photoelectron spectroscopies

ARTICLE *in* THE JOURNAL OF CHEMICAL PHYSICS · APRIL 2012

Impact Factor: 2.95 · DOI: 10.1063/1.3693271 · Source: PubMed

CITATIONS
2

READS
41

7 AUTHORS, INCLUDING:

Helen Gerardi
United States Naval Research Laboratory
7 PUBLICATIONS **20** CITATIONS
SEE PROFILE

Andrew F Deblase
Yale University
14 PUBLICATIONS **72** CITATIONS
SEE PROFILE

Xiaoge Su
University of Pittsburgh
5 PUBLICATIONS **27** CITATIONS
SEE PROFILE

Kenneth D Jordan
University of Pittsburgh
372 PUBLICATIONS **13,830** CITATIONS
SEE PROFILE

Available from: Andrew F Deblase
Retrieved on: 24 January 2016

Structural characterization of electron-induced proton transfer in the formic acid dimer anion, (HCOOH)2−, with vibrational and photoelectron spectroscopies

Helen K. Gerardi, Andrew F. DeBlase, Christopher M. Leavitt, Xiaoge Su, Kenneth D. Jordan et al.

Citation: J. Chem. Phys. **136**, 134318 (2012); doi: 10.1063/1.3693271
View online: http://dx.doi.org/10.1063/1.3693271
View Table of Contents: http://jcp.aip.org/resource/1/JCPSA6/v136/i13
Published by the AIP Publishing LLC.

Additional information on J. Chem. Phys.

Journal Homepage: http://jcp.aip.org/
Journal Information: http://jcp.aip.org/about/about_the_journal
Top downloads: http://jcp.aip.org/features/most_downloaded
Information for Authors: http://jcp.aip.org/authors

ADVERTISEMENT

Downloaded 22 Aug 2013 to 130.132.173.33. This article is copyrighted as indicated in the abstract. Reuse of AIP content is subject to the terms at: http://jcp.aip.org/about/rights_and_permissions

Structural characterization of electron-induced proton transfer in the formic acid dimer anion, $(HCOOH)_2^-$, with vibrational and photoelectron spectroscopies

Helen K. Gerardi,[1] Andrew F. DeBlase,[1] Christopher M. Leavitt,[1] Xiaoge Su,[2] Kenneth D. Jordan,[2] Anne B. McCoy,[3] and Mark A. Johnson[1,a)]
[1]*Sterling Chemistry Laboratory, Yale University, P.O. Box 208107, New Haven, Connecticut 06520, USA*
[2]*Department of Chemistry, University of Pittsburgh, Pittsburgh, Pennsylvania 15260, USA*
[3]*Department of Chemistry, The Ohio State University, Columbus, Ohio 43210, USA*

(Received 1 December 2011; accepted 17 February 2012; published online 5 April 2012)

The $(HCOOH)_2$ anion, formed by electron attachment to the formic acid dimer (FA_2), is an archetypal system for exploring the mechanics of the electron-induced proton transfer motif that is purported to occur when neutral nucleic acid base-pairs accommodate an excess electron [K. Aflatooni, G. A. Gallup, and P. D. Burrow, J. Phys. Chem. A **102**, 6205 (1998); J. H. Hendricks, S. A. Lyapustina, H. L. de Clercq, J. T. Snodgrass, and K. H. Bowen, J. Chem Phys. **104**, 7788 (1996); C. Desfrancois, H. Abdoul-Carime, and J. P. Schermann, *ibid.* **104**, 7792 (1996)]. The FA_2 anion and several of its H/D isotopologues were isolated in the gas phase and characterized using Ar-tagged vibrational predissociation and electron autodetachment spectroscopies. The photoelectron spectrum of the FA_2 anion was also recorded using velocity-map imaging. The resulting spectroscopic information verifies the equilibrium FA_2^- geometry predicted by theory which features a symmetrical, double H-bonded bridge effectively linking together constituents that most closely resemble the formate ion and a dihydroxymethyl radical. The spectroscopic signatures of this ion were analyzed with the aid of calculated anharmonic vibrational band patterns. © *2012 American Institute of Physics*. [http://dx.doi.org/10.1063/1.3693271]

I. INTRODUCTION

The accommodation of electrical charge by translocation of protons lies at the heart of many important chemical processes ranging from oxygen evolution in photosynthesis[2] to the radiation damage of DNA.[3] For example, several experimental studies involving electron impact on thin films of DNA (Ref. 4) have revealed that electrons with kinetic energies much lower than typical covalent bond energies can nonetheless induce single and double strand breaks. This effect has been explored with electronic structure calculations[5] as well as with experiments performed on isolated nucleic acid base-pairs,[6–8] and there is emerging consensus that the primary event in reductive DNA damage involves electron-induced proton transfer across multiple H-bond linkages. Here we explore the mechanics of this elementary process in a gas-phase spectroscopic study of the $(HCOOH)_2^-$ anion, FA_2^-. This system was chosen because the neutral formic acid dimer (FA_2), with the structure indicated in Fig. 1(a),[9] provides the simplest scaffold with the cyclic, multiple H-bonding motif found in the DNA base-pairs and because an earlier theoretical study by Bachorz *et al.*[10] concluded that formation of FA_2^- occurs through barrier-free intermolecular proton transfer.

In the present report, we first explore the electron binding behavior of FA_2^- to see if it is comparable to those reported for several gas-phase nucleic acid base-pair anions. This is carried out with velocity-map photoelectron imaging spectroscopy. We then obtain the vibrational spectrum of FA_2^- using a combination of Ar predissociation and electron autodetachment spectroscopies. Because many extra bands are observed due to strong intramolecular mode coupling, the unperturbed locations of fundamentals were recovered through extensive use of isotopic substitution. This required a survey of several isotopologues to isolate the various fundamentals across the spectrum by removing accidental degeneracies with background states. The assignments of the resulting band patterns were then determined through anharmonic analysis of the H/D isotope-dependence of the transitions, resulting in a microscopic picture of the H-bonding at play in the radical anion. The spectroscopic data confirms that the excess electron is accommodated by an intracluster proton transfer process.

It is useful to note at the outset that there are challenges in the generation of isolated, gas phase FA_2^-. Specifically, computational studies[10] indicate that, like the anions of isolated DNA bases,[1] FA_2^- is energetically unstable (by 0.4 kcal/mol or ~0.02 eV) with respect to spontaneous ejection of the electron, i.e., FA_2 has a negative adiabatic electron affinity (AEA). The calculated minimum energy structure of FA_2^- is shown in Fig. 1(b), which features a largely intact formate anion attached to a neutral dihydroxymethyl radical. The anion structure is quite different from the symmetrical structure of the neutral and, based on electronic structure calculations, it is anticipated that these two structures are separated by a substantial potential energy barrier (see diagram in Fig. 2). This is

a)Author to whom correspondence should be addressed. Electronic mail: mark.johnson@yale.edu.

 © 2012 American Institute of Physics

Downloaded 22 Aug 2013 to 130.132.173.33. This article is copyrighted as indicated in the abstract. Reuse of AIP content is subject to the terms at: http://jcp.aip.org/about/rights_and_permissions

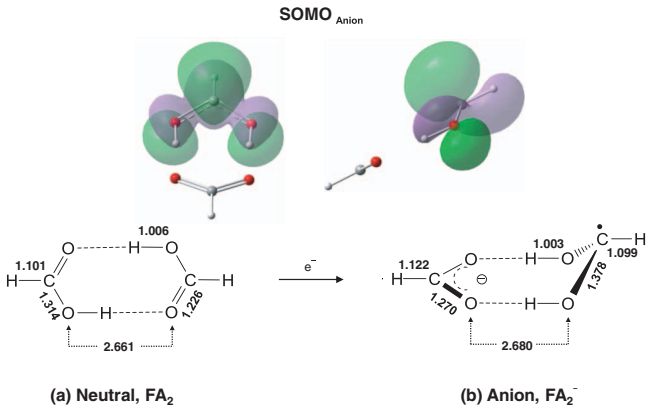

FIG. 1. Minimum energy structures (MP2/aug-cc-pVDZ level) of (a) the neutral formic acid dimer, FA_2, and (b) the radical anion formed by electron attachment, FA_2^-. Key geometrical parameters of these structures are indicated in angstroms (Å). Note the H–bond arrangement in the anion arises from transfer of one of the protons across the symmetrical bridge in the neutral dimer (C_{2h}) to form the dihydroxymethyl radical and formate ion (C_s). Two views of the singly occupied molecular orbital of FA_2^- ($SOMO_{Anion}$) in its equilibrium geometry are also shown.

important because it allows for the possibility that a metastable form of the anion can be isolated for study in the laboratory, analogous to the situation where the bent CO_2^- anion survives for ~90 μs before autodetaching the excess electron (in a tunneling mechanism) to form linear CO_2.[11]

Allan provided experimental support for this theoretical picture of the FA_2^- ion in a 2007 electron scattering study.[12] Specifically, he rationalized the quasithermalization of

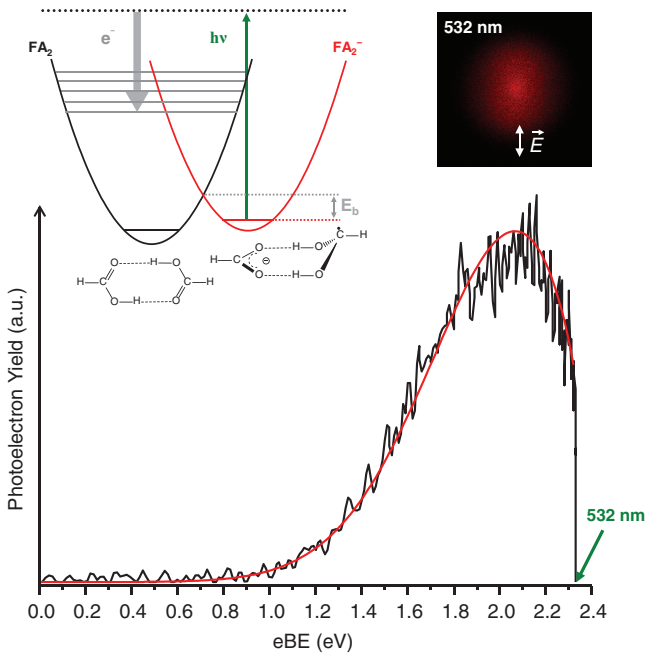

FIG. 2. Photoelectron spectrum of FA_2^- taken at 2.33 eV (532 nm) photon energy. The recorded image (top right) was (BASEX) (Ref. 33) transformed to yield the photoelectron spectrum displayed as the electron binding energy (eBE) distribution (black trace), which is not fully recovered at this photon energy. The red trace is a Gaussian function (FWHM = 0.67 eV) fit to the experimental data based upon a VDE value of 2.40 eV and accounting for suppression of photoelectrons near threshold assuming s-wave detachment, $(h\nu\text{-E(v)})^{1/2}$. The schematic potential energy diagrams (top left) emphasize the large change in geometry between FA_2 and FA_2^-.

1–2 eV electrons by neutral FA_2 in the context of a long-lived FA_2^- species formed by rapid, barrier-free intracluster proton transfer. This stabilization mechanism is the same as that invoked in excess electron accommodation by the isolated nucleic acid base-pairs mentioned above.[6,7]

The long-lived, transient FA_2^- anion, which has been invoked by Allan to explain the electron scattering results, provides an avenue for the gas-phase synthesis of FA_2^-, even if it is metastable, by quenching the nascent anion using an Ar-mediated electron attachment approach.[13]

$$(\mathrm{HCOOH})_2 \cdot \mathrm{Ar}_n + e^- \rightarrow (\mathrm{HCOOH})_2^- \cdot \mathrm{Ar}_m + (n-m)\mathrm{Ar}. \quad (1)$$

Since this process naturally incorporates Ar attachment in the product anion, we can then carry out its vibrational spectroscopic characterization by autodetachment of the bare anion as well as by Ar predissociation of the "tagged" species.[14] The latter is particularly useful since it lowers the internal energy content of the ion and allows us to focus on the properties of the vibrational zero-point system without complications from hot bands.

II. EXPERIMENTAL DETAILS

Anionic formic acid clusters were generated by passing approximately 4 atm of argon carrier gas over a ~8 °C reservoir containing 90% formic acid (with a balance of water) and expanding the mixture through the 0.5 mm-nozzle of a pulsed valve (Parker Hannifin, Series #9). The supersonic flow was ionized with a 1 keV counterpropagating electron beam, resulting in a distribution of formate and FA_2^- anions solvated by Ar, H_2O, and/or additional FA molecules. The $(\mathrm{HCOOD})_2^- \cdot \mathrm{Ar}$ mixed isotope species was synthesized by addition of deuterium oxide to the formic acid/H_2O mixture, while the perdeuterated species, $\mathrm{DCOOD}_2^- \cdot \mathrm{Ar}$, was formed by expanding a 16:1 mixture of argon and D_2 over 98% pure DCOOD (Sigma Aldrich), also held at ~8 °C.

Since the FA_2^- ion is metastable, we expect that the photoexcited ions will decay by both electron autodetachment and Ar loss. Vibrational spectra in the 600–3800 cm^{-1} range were therefore acquired for singly Ar-tagged parent anions by monitoring both fragmentation and electron ejection as a function of photon energy.[15] The branching ratio of these loss channels is governed by the relative magnitudes of the barrier to autodetachment (arising from the substantial rearrangement upon anion formation) and the Ar dissociation energy. In this case, Ar loss is kinetically favorable when available (vide infra), so that decomposition follows the sequence:

$$(\mathrm{HCOOH})_2^- \cdot \mathrm{Ar} + h\nu \rightarrow [(\mathrm{HCOOH})_2^- \cdot \mathrm{Ar}]^*, \quad (2)$$

$$[(\mathrm{HCOOH})_2^- \cdot \mathrm{Ar}]^* \rightarrow (\mathrm{HCOOH})_2^-[E_{\mathrm{int}}] + \mathrm{Ar}, \quad (3a)$$

$$(\mathrm{HCOOH})_2^-[E_{\mathrm{int}}] \rightarrow (\mathrm{HCOOH})_2 + e^-. \quad (3b)$$

This process can stop with an intact fragment ion (Eq. (3a)) provided its internal energy, E_{int}, falls below the barrier to autodetachment, E_b. As a result, the decomposition pathway generally evolves from fragmentation (Eq. (3a)) to electron detachment (Eq. (3b)) with increasing photon energy. This overall behavior is quite similar to that reported earlier

Downloaded 22 Aug 2013 to 130.132.173.33. This article is copyrighted as indicated in the abstract. Reuse of AIP content is subject to the terms at: http://jcp.aip.org/about/rights_and_permissions

for photodecomposition of Ar-tagged water cluster anions,[16] which also feature a very low AEA. When the AEA lies below the energies of vibrational fundamentals, the vibrational spectrum of bare FA_2^- can be monitored by autodetachment

$$(HCOOH)_2^- + h\nu \rightarrow (HCOOH)_2 + e^-, \quad (4)$$

which is especially useful because it allows us to directly quantify the extent to which the Ar tag perturbs the intrinsic structure of the ion.

These spectroscopic measurements were carried out using Yale's double-focusing, tandem time-of-flight photofragmentation mass spectrometer described in detail previously.[17] A tunable solid-state IR laser source (8 ns, 10 Hz Nd:YAG pumped Laser Vision OPO/OPA) provided photons in the 2500–3800 cm^{-1} range, while nonlinear mixing of the 1.5 and 3 μm outputs of the OPO/OPA in a $AgGaSe_2$ crystal extended the coverage down to 600 cm^{-1}. The reported spectra correspond to the addition of 5–15 individual scans and were corrected for laser pulse energy variation over the scan range. The FA_2^- photoelectron spectrum was recorded with the second harmonic (532 nm) of a Nd:YAG laser using a velocity-map imaging spectrometer.[18]

III. COMPUTATIONAL DETAILS

For the lowest energy FA_2^- structure, shown in Fig. 1(b), harmonic frequency calculations were completed using the GAUSSIAN 09 package[19] at the MP2/aug-cc-pVDZ level.[20] The vibrational energies obtained reproduce the values reported previously by Bachorz *et al.*[10] with the same level of theory and basis. The intensities in the harmonic spectra have been scaled in order to directly compare with the experimental action spectra. Specifically, the normal mode intensities were divided by the transition frequency to account for the fact that the experimental spectra were normalized to the laser power over the scan. This mode of presentation minimizes distortions due to very weak laser power available as the energy approaches the instrument cut-off at 600 cm^{-1}. In addition, anharmonic vibrational frequencies were calculated for FA_2^- and its isotopologues using second-order vibrational perturbation theory[21] exploiting force constants and harmonic frequencies computed at the MP2/aug-cc-pVDZ level of theory. These calculations were also performed using GAUSSIAN 09.

IV. RESULTS AND DISCUSSION

A. Photoelectron spectroscopy of FA_2^-

Figure 2 presents the raw image and photoelectron spectrum of FA_2^- at 2.33 eV (532 nm) excitation. The angular distribution is slightly skewed along the electric vector as might be anticipated from the complex shape of the SOMO depicted at the top of Fig. 1 for two orientations of the FA_2^-. The slowest electrons, however, adopt a more spherical profile as expected for suppression of the higher angular momentum partial waves near threshold. Unfortunately, the photon energy available for this study only allowed access to about half of the vibrational envelope and therefore the resulting spectrum appears as a broad feature with an abrupt drop to zero photoelectron yield at the laser excitation energy. While we could not directly obtain the eBE, we were able to determine that the recovered signal was consistent with a VDE value of 2.40 eV by simulating the photoelectron spectrum with a Gaussian distribution (FWHM = 0.67 eV) peaked at this value. With this simulation, we quantitatively recovered the experimental profile (see red trace in Fig. 2) with the anticipated cutoff due to s-wave threshold photoelectrons $\{(h\nu - EA(v))^{1/2}$, where v is the vibrational level of the neutral$\}$. Our experimental results thus support the theoretical 2.35 eV value and we note that this binding energy is within the range reported for several DNA nucleic acid base-pairs (1.9–2.6 eV).[6] Furthermore, the breadth of the band is consistent with the anticipated geometry change between the neutral formic acid dimer and the anion.

B. Survey of FA_2^- photophysics

Because the FA_2^- VDE (>2.33 eV) lies well above the region of its infrared fundamentals, vibrationally-mediated electron ejection (autodetachment) requires intramolecular vibrational redistribution (IVR) in order to generate configurations that approach the seam of intersections between the anionic and neutral potential surfaces.[22] The minimum energy of the seam, relative to the ground state of the ion, provides the barrier to autodetachment, E_b (Fig. 2), which has not been measured experimentally. We therefore first surveyed the electron photodetachment spectrum of bare FA_2^-, with the results displayed in Fig. 3(a). Very efficient photoinduced

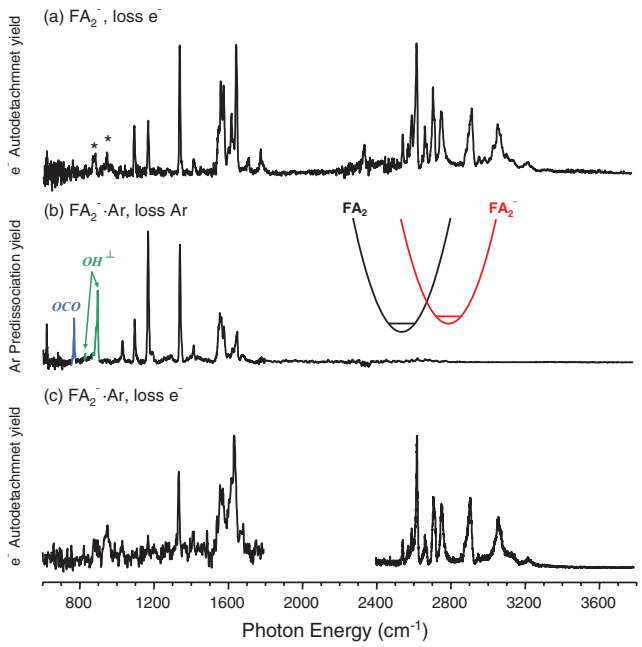

FIG. 3. Decay channel dependence of the FA_2^- vibrational spectrum: (a) the vibrational autodetachment of the bare formic acid dimer anion, FA_2^-, (b) Ar predissociation of $FA_2^- \cdot Ar$, and (c) autodetachment of $FA_2^- \cdot Ar$. In the case of $FA_2^- \cdot Ar$, photoexcitation below ~1000 cm^{-1} leads primarily to predissociation of the Ar tag while above ~1700 cm^{-1} electron autodetachment is the sole loss channel. The weak features (*) in trace (a) are likely due to vibrational hot band transitions of the ion.

Downloaded 22 Aug 2013 to 130.132.173.33. This article is copyrighted as indicated in the abstract. Reuse of AIP content is subject to the terms at: http://jcp.aip.org/about/rights_and_permissions

electron loss was observed throughout the higher energy range, but the yield falls off rapidly below ~1000 cm^{-1}, where the fundamental transitions associated with the O–C–O and O–H bending modes are expected to occur (green and blue at the left of Fig. 3(b)). This suggests that E_b lies close to this cut-off, which would suppress detection of bands below E_b. We note, however, that because the bare ion likely retains internal energy prior to photoexcitation, this cut-off actually represents a lower bound on E_b.

To observe the vibrational transitions below the autodetachment cut-off, we turn to the Ar-tagged species, $FA_2^- \cdot Ar$. Since an Ar atom is typically bound to anions by only a few hundred cm^{-1},[23] the expected fundamental resonances (which all occur at energies greater than the Ar binding energy) should be observable by detecting the bare FA_2^- ion resulting from Ar dissociation. The fragmentation spectrum is presented in Fig. 3(b). The region from 1100 to 1600 cm^{-1} displays the same transitions (to within the laser bandwidth) as those found in the bare anion, but also reveals many strong bands down to the lower limit of the laser at 600 cm^{-1}, including the O–C–O and perpendicular O–H bends. The low-energy cut off in the photodetachment spectrum supports the conclusion that the barrier to electron ejection lies near 1000 cm^{-1}. Note that the weak bands labeled "*" in Fig. 3(a), which fall below 1000 cm^{-1} in the autodetachment spectrum of the bare ion, are narrower or missing in the Ar predissociation spectrum. These unusual features likely result from vibrational hot band activity in a scenario where excitation of population in a vibrationally excited level brings the system above E_b even when the photon energy is not itself sufficient to induce electron ejection. We emphasize that the similarities of the strong resonances (when they appear in both spectra) establish that the Ar atom does not significantly perturb the structure of the ion.

Interestingly, the predissociation spectrum (Fig. 3(b)) also displays a cut-off effect in which bands *above* 1500 cm^{-1} or so are suppressed. This is expected, however, as the nascent FA_2^- product ion (after Ar loss from the parent ion, $FA_2^- \cdot Ar$) retains significant internal energy, $E_{int} \sim h\nu - D_0(Ar)$. When this energy exceeds E_b, the anion will also decay by electron ejection (Eq. (3b)). Thus, one expects the onset of vibrational autodetachment in the Ar-tagged species to be displaced to higher wavenumbers by roughly the energy carried away by the Ar dissociation event. We therefore also monitored the electron loss channel for the $FA_2^- \cdot Ar$ ion, with the result displayed in Fig. 3(c). The "missing" bands in the fragmentation spectrum all appear in the photodetachment channel, again with positions almost identical to those found in the bare ion (trace Fig. 3(a)). As such, the reported bands in what follows are a combination of those observed in autodetachment of bare FA_2^- above 1000 cm^{-1} and Ar predissociation of $FA_2^- \cdot Ar$ below that energy.

In the event that the internal energy content of the bare and Ar-tagged species is comparable, the displacement of the electron autodetachment onset from 1000 cm^{-1} in the bare ion to ~1350 cm^{-1} in $FA_2^- \cdot Ar$ is consistent with an effective Ar binding energy of about 350 cm^{-1}, which is typical for Ar attachment to negative ions in this size range.[23]

C. Assignment of the vibrational transitions in the FA_2^- spectrum in the C–O stretching region

The calculated structure of the formic acid dimer anion (Fig. 1(b)) indicates that it can be viewed as a binary complex between the formate ion, HCO_2^-, and the dihydroxymethyl radical, $HC(OH)_2^{\bullet}$, which are bound by a double H-bond bridge. Based on this equilibrium structure, we began the analysis of the FA_2^- vibrational spectrum by seeking the spectral signatures of each component in the region of heavy atom motions largely associated with the skeletal framework of the complex (600–1800 cm^{-1}). Specifically, while only two O–C–O-based transitions (derived from collective O–C–O symmetric and asymmetric stretches) are IR-active in the high symmetry (C_{2h}), neutral FA_2 system, these modes should split into four allowed and distinct bands due to the lower C_s symmetry of the anion.

Figure 4 compares the low energy Ar predissociation spectra of $FA_2^- \cdot Ar$ (see below) and $HCO_2^- \cdot Ar$ (reported earlier, Fig. 4(a)),[24] with the calculated harmonic spectrum (Fig. 4(c)) for the FA_2^- structure displayed in Fig. 1(b). The O–C–O stretches associated with the dihydroxymethyl radical component, $\nu_{COs}^{radical}$ and $\nu_{COa}^{radical}$, highlighted in dark blue, are centered around 1150 cm^{-1} and are very similar to those predicted for the ion-radical structure (see Table I). The formate constituent, on the other hand, does not behave as expected. Whereas the calculated spectrum features two bands (indicated in red) very close to the asymmetric ($\nu_{COa}^{formate}$) and symmetric ($\nu_{COs}^{formate}$) O–C–O stretches found in the isolated

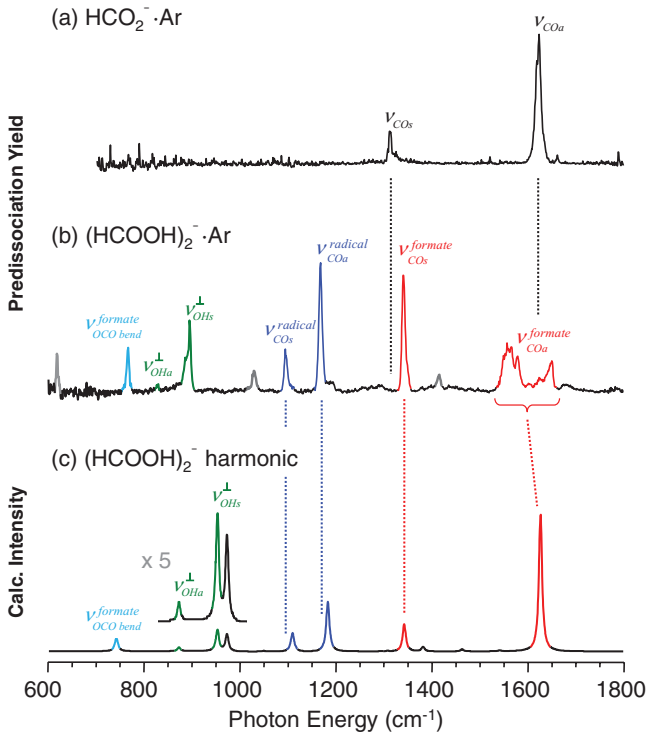

FIG. 4. Comparison of the Ar predissociation spectra of (a) $HCO_2^- \cdot Ar$ and (b) $(HCOOH)_2^- \cdot Ar$, along with (c) the calculated harmonic spectrum of $(HCOOH)_2^-$. The color-coded peaks correspond to assigned features with positions collected in Table I. We note that the spectrum in (a) was previously reported in Ref. 24.

Downloaded 22 Aug 2013 to 130.132.173.33. This article is copyrighted as indicated in the abstract. Reuse of AIP content is subject to the terms at: http://jcp.aip.org/about/rights_and_permissions

TABLE I. Experimental (±6 cm^{-1}) and calculated band positions of the $(HCOOH)_2^-$ and $(DCOOD)_2^-$ isotopologues in the fingerprint region, 600–1800 cm^{-1}.

Species	Method[a]	Frequencies (cm^{-1})							
		$\nu_{OH/ODa}^{\perp}$	$\nu_{OCO\ bend}$	$\nu_{OH/ODs}^{\perp}$	$\nu_{CH/CD\ ip\ bend}^{radical}$	$\nu_{COs}^{radical}$	$\nu_{COa}^{radical}$	$\nu_{COs}^{formate}$	$\nu_{COa}^{formate}$
$(HCOOH)_2^-$	Harmonic	872	741	953	1307	1109	1183	1342	1627
	Anharmonic	822	734	903	1270	1085	1147	1320	1581
$(HCOOH)_2^- \cdot Ar$	Experimental	829	765	893	...	1094	1168	1341	1561/1651
$(DCOOD)_2^-$	Harmonic	627	742	688	938	1066	1225	1320	1614
	Anharmonic	597	729	659	920	1038	1177	1300	1581
$(DCOOD)_2^- \cdot Ar$	Experimental	...	769	663	929	1040	1212	1321	1599

[a]Calculations were performed using the MP2/aug-cc-pVDZ method. The anharmonic frequencies were calculated using the VPT2 method.

formate ion (Fig. 4(a)), only the lower energy symmetric stretch (at 1341 cm^{-1}) appears as a distinct band in the experimental FA_2^- spectrum. The region near the predicted location of the asymmetric $\nu_{COa}^{formate}$ transition exhibits a broad multiplet structure, with weaker bands spanning the range between stronger peaks at the extremes of the feature. We suspect that this suite of bands in the experimental spectrum derives from extensive mixing of the O–C–O asymmetric stretch fundamental in the formate component with combinations and overtones of lower energy modes. This behavior is consistent with the strong coupling typically encountered when H-bonds are in play.[25]

A simple way to test whether the splitting and degradation of the oscillator strength associated with the $\nu_{COa}^{formate}$ fundamental in the $(HCOOH)_2^-$ isotopologue is due to the v = 1 level of this oscillator coupling to other vibrational modes is to extend the study to the $(DCOOD)_2^-$ species in the hope of removing such accidental degeneracies. The result is displayed in Fig. 5(b), again along with the calculated harmonic spectrum (Fig. 5(c)) and the experimental spectrum of $DCO_2^- \cdot Ar$ (Fig. 5(a)). Most notable is that the experimental $(DCOOD)_2^-$ spectrum reveals both the symmetric ($\nu_{COs}^{formate}$) and asymmetric ($\nu_{COa}^{formate}$) stretching O–C–O vibrations with their locations and relative intensities closely matching those of bare formate and the predicted behavior of the dimer anion. In addition, the O–C–O fundamentals of the dihydroxymethyl radical component ($\nu_{COs}^{radical}$ and $\nu_{COa}^{radical}$, blue) are clearly evident at 1040 cm^{-1} and 1212 cm^{-1}, and remain in close agreement with the calculated harmonic frequencies for these modes at 1066 and 1225 cm^{-1}, respectively. We therefore conclude that the formate-dihydroxymethyl species, with the structure presented in Fig. 1(b), is indeed formed when the nascent FA_2^- ion is quenched into its local minimum. Table I summarizes the band assignments for both the $(HCOOH)_2^-$ and $(DCOOD)_2^-$ species in the lower energy region while Table II compares experimental and calculated values of the O–C–O stretches in the isolated constituents (formate, DCO_2^- and the dihydroxymethyl radical, $DCOOD_2^{\bullet}$).

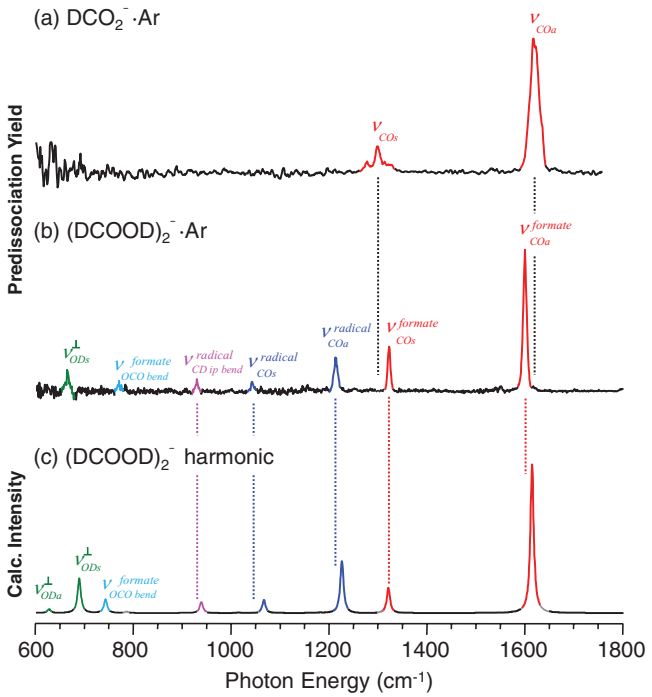

FIG. 5. Comparison of the Ar predissociation spectra of (a) $DCO_2^- \cdot Ar$ and (b) $(DCOOD)_2^- \cdot Ar$, along with (c) the calculated harmonic spectrum of $(DCOOD)_2^-$. The positions of color-coded bands are collected in Table I. We note that the spectrum in (a) was previously reported in Ref. 24.

D. Assignment of C–H modes and motions involving the bridging O–H groups in FA_2^-

In addition to the O–C–O stretches, the other clear signatures associated with the symmetry-breaking in FA_2 upon electron attachment are the frequencies of the C–H stretches located at the exterior of the complex. In the symmetrical neutral dimer, the latter modes are collective in nature and are

TABLE II. O–C–O fundamental transitions of the isolated FA_2^- components DCO_2^- and $DC(OD)_2^{\bullet}$.

Components	Mode	Method[a]		
		Harmonic (cm^{-1})	Anharmonic (cm^{-1})	Experimental (cm^{-1})
DCO_2^-	$\nu_{COa}^{formate}$	1627	1600	1616
	$\nu_{COs}^{formate}$	1311	1288	1298
$DC(OD)_2^{\bullet}$	$\nu_{COa}^{radical}$	1172	1205	...
	$\nu_{COs}^{radical}$	1090	1109	...

[a]Calculations were performed using the MP2/aug-cc-pVDZ method. The anharmonic frequencies were calculated using the VPT2 method. Experimental energies (±6 cm^{-1}) are from Ar predissociation spectroscopy of $DCO_2^- \cdot Ar$.

Downloaded 22 Aug 2013 to 130.132.173.33. This article is copyrighted as indicated in the abstract. Reuse of AIP content is subject to the terms at: http://jcp.aip.org/about/rights_and_permissions

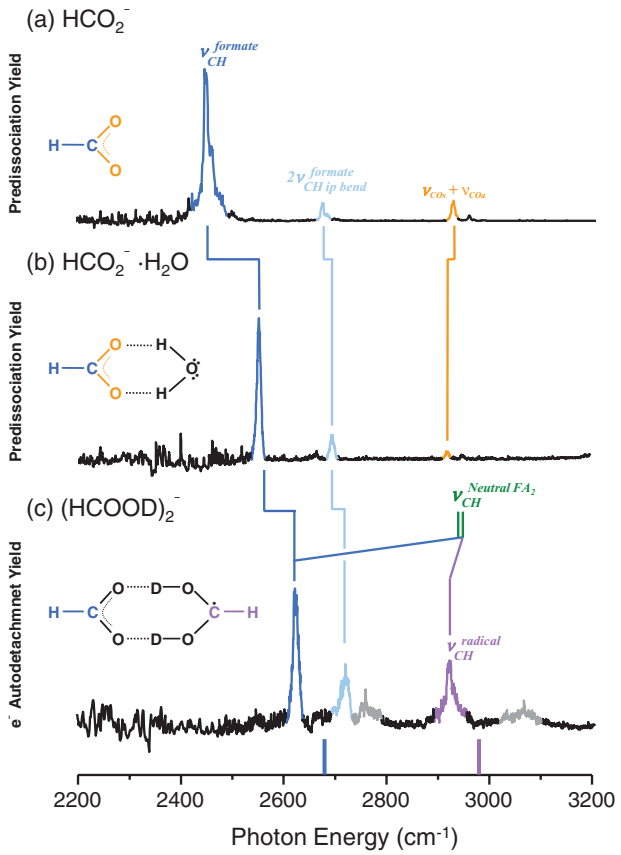

FIG. 6. Evolution of the CH stretch from the point-of-view of FA_2^- as a solvated formate ion: Ar predissociation spectra of (a) $HCO_2^- \cdot Ar$, (b) $HCO_2^- \cdot H_2O \cdot Ar$, and (c) the electron autodetachment spectrum of $(HCOOD)_2^-$. The lines below trace (c) indicate the anharmonic positions (VPT2, see text) of the formate CH and neutral radical CH stretch fundamentals in the $(HCOOD)_2^-$ complex, while the green lines indicate the CH stretching fundamentals in neutral FA_2.

nearly degenerate around ~2950 cm^{-1} (labeled $\nu_{CH}^{Neutral\,FA_2}$, green lines at the right in Figure 6(c)),[26] but should evolve into two distinct C–H stretching frequencies in the anion (one localized on each component). For the FA_2^- constituent derived from the formate ion, we expect a very low-energy C–H stretch fundamental based on the vibrational energy of this mode in Ar-tagged HCO_2^- (at 2452 cm^{-1} in Fig. 6(a)).[24] There is a complication, however, as the $\nu_{CH}^{formate}$ fundamental is anomalously responsive to its local solvation environment. For example, complexation with a single water molecule blue-shifts the CH stretch by over 100 cm^{-1},[24] and in aqueous solution the band appears near 2830 cm^{-1},[27] representing a solvent shift of about 400 cm^{-1}. We therefore anticipate that, in the case of FA_2^-, solvation of the embedded formate ion by the dihydroxymethyl radical will induce a significant blue-shift in the C–H stretch of the formate component relative to that of the fundamental in the isolated anion.

To gauge the FA_2^- behavior in the context of solvation, Fig. 6 presents the evolution of $\nu_{CH}^{formate}$ (highlighted in dark blue) from HCO_2^- (Fig. 6(a)) to the monohydrate (Fig. 6(b)) and then to FA_2^- (Fig. 6(c)). Because the higher frequency (O–H and C–H) stretches are also heavily perturbed by accidental degeneracies and intermolecular couplings, we chose to focus here on the $(HCOOD)_2^-$ isotopomer (i.e. with terminal C–H groups) that minimizes these effects. The anharmonic predictions for the two FA_2^- C–H stretches ($\nu_{CH}^{formate}$ in dark blue and $\nu_{CH}^{radical}$ in purple) are indicated with the color-coded scheme at the bottom of Fig. 6(c). The anharmonic $\nu_{CH}^{formate}$ value falls between the observed lines at 2620 cm^{-1} (dark blue) and 2718 cm^{-1} (light blue), which are close to an analogous pair in the monohydrate. In the latter system, these two transitions were analyzed in the context of a simple 2×2 Fermi resonance interaction between the $\nu_{CH}^{formate}$ fundamental and the overtone of the in-plane CH bending mode ($\nu_{CH\,ip\,bend}^{formate}$).[24] The C–H stretch is thus found to blue-shift by 168 cm^{-1} from bare formate to FA_2^-, with the dihyroxymethyl group inducing about 100 cm^{-1} larger solvent shift than a water molecule. Because the C–H bend frequency is not strongly solvent-dependent, the blue-shifting C–H stretch fundamental (from isolated HCO_2^- to FA_2^-) becomes increasingly mixed as it approaches accidental degeneracy with $2\nu_{CH\,ip\,bend}^{formate}$. Since the oscillator strength of the bend overtone is small, $2\nu_{CH\,ip\,bend}^{formate}$ appears through intensity borrowing from the stretch, and hence becomes more pronounced as this mixing is increased in FA_2^-.

Turning to the C–H stretch of the neutral radical component of the complex ($\nu_{CH}^{radical}$), the anharmonic calculations predict the transition to occur at 2977 cm^{-1} with an intensity, from the harmonic calculation, about three times weaker than $\nu_{CH}^{formate}$. The observed spectrum displays a feature at 2918 cm^{-1}, with intensity less than half that of the experimental $\nu_{CH}^{formate}$ band, following the predicted trend reasonably well. Although the latter band overlaps with the $\nu_{COa} + \nu_{COs}$ combination band (orange in Figs. 6(a) and 6(b)) derived from the formate component, its intensity is much larger in the $(HCOOD)_2^-$ isotopologue, consistent with a major contribution from the radical C–H stretch fundamental.

The situation regarding the spectral signatures of the bridging hydrogen atoms is more complex. Figure 7 presents the evolution of the O–H(D) and C–H(D) stretches for three isotopologues. The main band assignments are highlighted with the same color scheme as in Fig. 6 with the addition of red indicating the O–H(D) stretches. Selected values are collected in Table III. While extra bands appear in all three systems beyond what is expected for fundamentals and for the C–H(D) stretch/bend Fermi resonance, the isotope dependence of the band patterns does reveal several persistent features that can be assigned with confidence. In particular, the $\nu_{CH}^{formate}$ (dark blue), $2\nu_{CH\,ip\,bend}^{formate}$ (light blue), and $\nu_{CH}^{radical}$ (purple) transitions isolated in Fig. 6 are clearly present in the more complex $(HCOOH)_2^-$ spectrum (Fig. 7(a)) and this characteristic pattern is readily identified among the many bands in the $(DCOOD)_2^-$ isotopologue.

The $(HCOOD)_2^-$ species presents the most straightforward assignment of the O–D stretches as the 2148 cm^{-1} feature (highlighted in red in Fig. 7(b)) appears in a relatively isolated region when D atoms are placed in both bridging positions, and this band persists in the $(DCOOD)_2^-$ spectrum (Fig. 7(c)). Although there appear to be contributions from several of the isotopomers with two H and two D atoms in the various possible positions, the $(HCOOD)_2^-$ isotopomer dominates based on the behavior of the C–H(D) band

Downloaded 22 Aug 2013 to 130.132.173.33. This article is copyrighted as indicated in the abstract. Reuse of AIP content is subject to the terms at: http://jcp.aip.org/about/rights_and_permissions

TABLE III. Experimental (±6 cm^{-1}) and calculated band positions tabulated for the $(HCOOH)_2^-$, $(HCOOD)_2^-$, and $(DCOOD)_2^-$ isotopologues through the OH/OD and CH/CD stretching regions.

Species	Method[a]	Frequency (cm^{-1})				
		ν_{OD}	$\nu_{CH/CD}^{formate}$	$2\nu_{CH/CD\ ip\ bend}^{formate}$	$\nu_{CH/CD}^{radical}$	ν_{OH}
$(HCOOH)_2^-$	Harmonic	…	2884	…	3118	3186
	Anharmonic	…	2673	2784	2938	3030
	Experimental	…	2621	2717	2913	3061
$(HCOOD)_2^-$	Harmonic	2308	2884	…	3132	…
	Anharmonic	2127	2676	2782	2977	…
	Experimental	2144	2621	2717	2918	…
$(DCOOD)_2^-$	Harmonic	2329	2120	…	2296	…
	Anharmonic	2195	2057	1988	2146	…
	Experimental	2148	1969	2026	2081	…

[a]Calculations were performed using the MP2/aug-cc-pVDZ method. The anharmonic frequencies were calculated using the VPT2 method for bare $(HCOOH)_2^-$, $(HCOOD)_2^-$, and $(DCOOD)_2^-$ and are compared to experimental transitions recorded in the photodetachment spectra of the $(HCOOH)_2^-$, $(HCOOD)_2^-$, and $(DCOOD)_2^-$ species.

structure. The $(HCOOD)_2^-$ species with the arrangement indicated in the inset of Fig. 7(b) is clearly most informative regarding the signature of the bridging H-bonds as the O–D stretches are largely decoupled from the C–H stretches as well as the combination band arising from simultaneous excitations of the $\nu_{COa} + \nu_{COs}$ modes on the formate constituent (orange in Fig. 7(c)). The isolated O–D stretches are quite simple, and the close doublet structure of the red feature in Figs. 7(b) and 7(c) is consistent with the expected splitting due to the symmetric and asymmetric stretches of the nominally symmetrical O–D bonds in the ion-radical complex. The calculations predict that in the homogeneous isotopologues, the bridging O–H(D) and exterior C–H(D) stretches are highly coupled such that the symmetric O–H(D) stretch combines in- and out-of-phase with the C–H(D) oscillator. This would partially explain the more complex structure in the $(HCOOH)_2^-$ and $(DCOOD)_2^-$ systems, and warrants further analysis with careful isolation of particular isotopomers in the mixed isotopologues. While more sophisticated theoretical analysis would be needed to fully unravel all the Fermi interactions present in these spectra, the persistent bands across the three species allow a secure identification of the basic structure of the FA_2^- ion as well as clarify the overall signatures of the various motions associated with the H-bonded ion-radical motif.

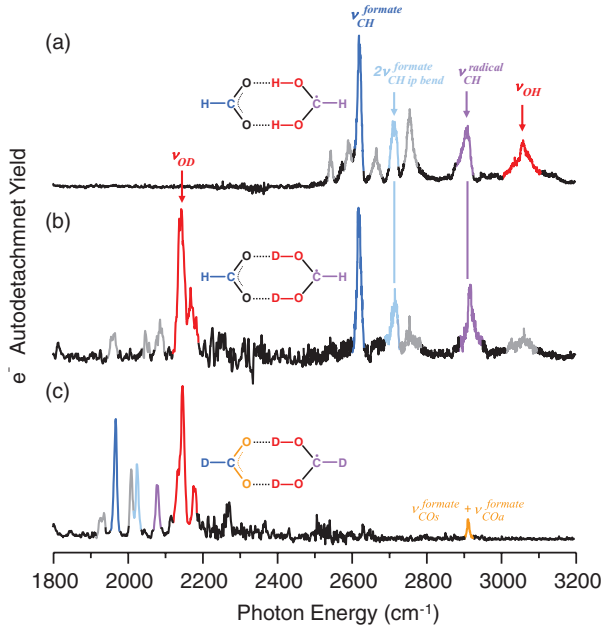

FIG. 7. Vibrational spectra of (a) $(HCOOH)_2^-$, (b) $(HCOOD)_2^-$, and (c) $(DCOOD)_2^-$. Bands are color-coded, referring to fundamentals derived from motions of the atoms indicated in the inset structures. The peaks highlighted in grey in traces (a) and (c) are likely due to extensive intramolecular mode couplings. In trace (b), minor contributions to the spectrum could also arise from contamination by various mass-degenerate isotopologues. The energy values of the labeled bands are provided in Table III.

V. SUMMARY

The bare and Ar-tagged negative ions of the formic acid dimer have been synthesized using Ar cluster-mediated electron attachment to the neutral formic acid dimer. Photoelectron spectroscopy supports the predicted vertical detachment energy (2.35 eV) of the anion.[10] Sharp vibrational bands were observed for several FA_2^- isotopologues using a combination of electron autodetachment and Ar predissociation spectroscopies. The spectrum was deconvoluted through strategic isotopic substitution that revealed a structure composed of a largely intact formate ion attached to the dihydroxymethyl radical through a symmetrical, double O–H bonded bridge. From these results, we conclude that electron attachment occurs with barrier-free transfer of one of the protons across the H-bond bridge upon formation of the radical anion as computationally predicted by Bachorz *et al.*[10] and supported by the inelastic electron scattering results of Allan.[12] Once formed, the anion is locally stable as substantial geometrical rearrangement is required to reach the lowest energy seam connecting the anion to the neutral surface.

ACKNOWLEDGMENTS

M.A.J. and K.D.J. would like to thank the Department of Energy under grants DE-FG02-00ER15066 and DE-FG02-06ER15800 for support of this work and A.B.M. would like to thank the National Science Foundation under grant CHE-0848242.

Downloaded 22 Aug 2013 to 130.132.173.33. This article is copyrighted as indicated in the abstract. Reuse of AIP content is subject to the terms at: http://jcp.aip.org/about/rights_and_permissions

[1]K. Aflatooni, G. A. Gallup, and P. D. Burrow, J. Phys. Chem. A **102**, 6205 (1998); J. H. Hendricks, S. A. Lyapustina, H. L. de Clercq, J. T. Snodgrass, and K. H. Bowen, J. Chem. Phys. **104**, 7788 (1996); C. Desfrancois, H. Abdoul-Carime, and J. P. Schermann, *ibid.* **104**, 7792 (1996).
[2]G. Renger, Biochim. Biophys. Acta **1655**, 195 (2004).
[3]Z. Cai and M. D. Sevilla, *Long-Range Charge Transfer in DNA II*, edited by G. B. Schuster (Springer, 2004), Vol. 237, p. 103.
[4]B. Boudaiffa, P. Cloutier, D. Hunting, M. A. Huels, and L. Sanche, Science **287**, 1658 (2000); F. Martin, P. D. Burrow, Z. Cai, P. Cloutier, D. Hunting, and L. Sanche, Phys. Rev. Lett. **93**, 068101 (2004).
[5]R. Barrios, P. Skurski, and J. Simons, J. Phys. Chem. B **106**, 7991 (2002); M. Gutowski, I. Dabkowska, J. Rak, S. Xu, J. M. Nilles, D. Radisic *et al.*, Eur. Phys. J. D **20**, 431 (2002); X. Li, M. D. Sevilla, and L. Sanche, J. Am. Chem. Soc. **125**, 13668 (2003); I. Dabkowska, J. Rak, and M. Gutowski, Eur. J. Phys. D **35**, 429 (2005); C. E. Hamilton, J. L. Kinsey, and R. W. Field, Ann. Rev. Phys. Chem. **37**, 493 (1986).
[6]A. Szyperska, J. Rak, J. Leszczynski, X. Li, Y. J. Ko, H. Wang *et al.*, J. Am. Chem. Soc. **131**, 2663 (2009); A. Szyperska, J. Rak, J. Leszczynski, X. Li, Y. J. Ko, H. Wang *et al.*, ChemPhysChem **11**, 880 (2010).
[7]E. Nir, K. Kleinermanns, and M. S. de Vries, Nature **408**, 949 (2000); I. Dabkowska, J. Rak, M. Gutowski, J. M. Nilles, S. T. Stokes, D. Radisic *et al.*, Phys. Chem. Chem. Phys. **6**, 4351 (2004).
[8]D. Radisic, K. H. Bowen, I. Dabkowska, P. Storoniak, J. Rak, and M. Gutowski, J. Am. Chem. Soc. **127**, 6443 (2005).
[9]S. Scheiner and C. W. Kern, J. Am. Chem. Soc. **101**, 4081 (1979); S. Kishida and K. Nakamoto, J. Chem. Phys. **41**, 1558 (1964); E. Clementi, J. Mehl, and W. von Niessen, J. Chem. Phys. **54**, 508 (1971).
[10]R. A. Bachorz, M. Haranczyk, I. Dabkowska, J. Rak, and M. Gutowski, J. Chem. Phys. **122**, 204304 (2005).
[11]J.-W. Shin, N. I. Hammer, M. A. Johnson, H. Schneider, A. Gloss, and J. M. Weber, J. Phys. Chem. A **109**, 3146 (2005); R. N. Compton, P. W. Reinhardt, and C. D. Cooper, J. Chem. Phys. **63**, 3821 (1975).
[12]M. Allan, Phys. Rev. Lett. **98**, 123201 (2007).
[13]M. A. Johnson and W. C. Lineberger, *Techniques for the Study of Ion-Molecule Reactions*, edited by J. M. Farrar and W. H. Saunders, Jr. (Wiley, 1988), Vol. XX, p. 591.
[14]C. E. Klots, J. Chem. Phys. **83**, 5854 (1985); P. Ayotte, G. H. Weddle, J. Kim, and M. A. Johnson, J. Am. Chem. Soc. **120**, 12361 (1998); P. Ayotte, J. Kim, J. A. Kelley, S. B. Nielsen, and M. A. Johnson, J. Am. Chem. Soc. **121**, 6950 (1999); E. J. Bieske and O. Dopfer, Chem. Rev. **100**, 3963 (2000); J. M. Weber, J. A. Kelley, S. B. Nielsen, P. Ayotte, and M. A. Johnson, Science **287**, 2461 (2000); D. M. Neumark, K. R. Lykke, T. Andersen, and W. C. Lineberger, J. Chem. Phys. **83**, 4364 (1985).
[15]H. K. Gerardi, K. J. Breen, T. L. Guasco, G. H. Weddle, G. H. Gardenier, J. E. Laaser *et al.*, J. Phys. Chem. A **114**, 1592 (2010).
[16]B. M. Elliott, L. R. McCunn, and M. A. Johnson, Chem. Phys. Lett. **467**, 32 (2008).
[17]L. A. Posey and M. A. Johnson, J. Chem. Phys. **89**, 4807 (1988).
[18]A. T. J. B. Eppink and D. H. Parker, Rev. Sci. Instrum. **68**, 3477 (1997); V. Dribinski, A. Ossadtchi, V. A. Mandelshtam, and H. Reisler, *ibid.* **73**, 2634 (2002); A. Sanov and R. Mabbs, Int. Rev. Phys. Chem. **27**, 53 (2008).
[19]M. J. Frisch, G. W. Trucks, H. B. Schlegel *et al.*, GAUSSIAN 09, Revision A.02 (Gaussian, Inc., Wallingford, CT, 2009).
[20]T. H. Dunning, Jr., J. Chem. Phys. **90**, 1007 (1989); R. A. Kendall, T. H. Dunning, Jr., and R. J. Harrison, *ibid.* **96**, 6796 (1992).
[21]V. Barone, J. Chem. Phys. **122**, 014108 (2005).
[22]C. L. Adams, H. Schneider, K. M. Ervin, and J. M. Weber, J. Chem. Phys. **130**, 074307 (2009).
[23]J. H. Hendricks, H. L. de Clercq, C. B. Freidhoff, S. T. Arnold, J. G. Eaton, C. Fancher *et al.*, J. Chem. Phys. **116**, 7926 (2002); H. Schneider, K. Takahashi, R. T. Skodje, and J. M. Weber, *ibid.* **130**, 174302 (2009).
[24]H. K. Gerardi, A. F. DeBlase, X. Su, K. D. Jordan, A. B. McCoy, and M. A. Johnson, J. Phys. Chem. Lett. **2**, 2437 (2011).
[25]J. R. Roscioli, L. R. McCunn, and M. A. Johnson, Science **316**, 249 (2007).
[26]R. Georges, M. Freytes, D. Hurtmans, I. Kleiner, J. Vander Auwera, and M. Herman, Chem. Phys. **305**, 187 (2004).
[27]K. G. Kidd and H. H. Mantsch, J. Mol. Spectrosc. **85**, 375 (1981).

Downloaded 22 Aug 2013 to 130.132.173.33. This article is copyrighted as indicated in the abstract. Reuse of AIP content is subject to the terms at: http://jcp.aip.org/about/rights_and_permissions